*Journal of*
*Computational and Theoretical Nanoscience*
Vol. 7, 1–5, 2010

# *Ab Initio* Study of Hydrogen Storage in Water Clathrates

Jacalyn S. Clawson†, Randall T. Cygan, Todd M. Alam, Kevin Leung, and Susan B. Rempe*

*Sandia National Laboratories, Albuquerque, NM 87185 USA*

The $H_2$ occupancy in type-II hydrogen clathrate is determined using *ab initio* quantum chemistry calculations. Free energies of association show that the small (D-$5^{12}$) cage is singly occupied while the large (H-$5^{12}6^4$) favors a four-fold occupancy.

**Keywords:** Clathrate, Hydrogen Storage, *Ab Initio* Quantum Chemical Calculations.

## 1. INTRODUCTION

Since the first hydrogen water clathrates were synthesized,[1] much attention has been placed on them as a means of storing $H_2$ for fuel.[2] The type II hydrogen clathrate contains 136 water molecules consisting of 24 cages. Sixteen of these cages have a "small" pentagonal dodecahedral (D-$5^{12}$) structure, while the remaining cages are in a "large" 16-hedra (H-$5^{12}6^4$) structure. Initial reports demonstrated a 5.3% mass storing capacity, above the 2005 DOE target (4.5 wt%) of $H_2$ fuel storage. Because of this large capacity, the distribution of the $H_2$ molecules through these cages has been the emphasis of several works. Initial studies showed two guest $H_2$ molecules occupying the small cages while four guest $H_2$ molecules were stored in the large cage.[3,4] Recent experimental[5] and theoretical molecular dynamics (MD) simulations,[6] however, suggested that only one $H_2$ molecule is stored in the small cage, thereby reducing the mass ratio to 3.9 wt%. This work will reinvestigate the hydrogen storage in type-II hydrate clathrates using *ab initio* quantum chemical calculations.

## 2. COMPUTATIONAL DETAILS

The oxygen positions of the water cages were obtained from X-ray structure for the type-II hydrated clathrates.[7] The hydrogen bonding network, not available from the scattering data, was generated using classical force field simulations.[8] The hydrate geometry and lattice constants for a single unit cell were then relaxed using the plane-wave based Vienna *ab initio* simulation package (VASP),[9–11] the generalized gradient approximation (GGA) of Perdew-Wang[12–16] (PW91), ultrasoft Vanderbilt pseudopotentials,[17] gamma-point Brillouin sampling, and a 400 eV kinetic energy cut-off for the plane-wave expansion of the valence electronic wave functions.

Two cages, one small (D-$5^{12}$) and one large (H-$5^{12}6^4$), were extracted randomly from the optimized type II clathrate unit cell and free energy calculations for various $H_2$ loadings were performed. The DFT energy calculations on these isolated clusters employed the GAUSSIAN 03 software package.[18] $H_2$ occupancies of one to three and one to five were considered for the small and large cages, respectively. In all cases the guest $H_2$ molecules were fully optimized in these fixed cages using a restricted Becke's three-parameter hybrid functional[19] with the Lee, Yang, and Par correlation functional[20] (rB3LYP) and the 6-311G[21,22] basis set. For each optimization at least two different starting positions were considered to ensure that a global minimum had been reached. Single point energy calculations were performed using the second-order Möller Plesset (MP2)[23] wave functions. To determine the minimum basis set, association free energy calculations were performed on the small (D-$5^{12}$) cage with one to three guest $H_2$ molecules using increasingly larger basis sets until a convergence in energy was realized: 3-21G[24–29], 6-311G, 6-311G*, 6-311G**, 6-311+G* to 6-311++G**. Association energies of the large (H-$5^{12}6^4$) cage were calculated using this minimum basis set.

The energies for association of hydrogen molecules with large and small cages in the type-II clathrate were calculated by considering the following reactions:

$$n\mathrm{H_2} + \mathrm{Cage} \rightarrow n\mathrm{H_2}@\mathrm{Cage}, \quad \text{and}$$
$$\Delta E = \{E(n\mathrm{H_2}@\mathrm{Cage}) - [E(n\mathrm{H_2}) + E(\mathrm{Cage})]\} - nRT\ln(P/P_0), \quad (1)$$

where $n$ is the number of guest $H_2$ molecules, $E$(Cage) is the energy of the rigid cage, $E(n\mathrm{H_2})$ is the energy of

*Author to whom correspondence should be addressed.
†Current address: GlaxoSmithKline Plc, Preclin Dev, King of Prussia, PA 19406 USA.

RESEARCH ARTICLE

$n$ optimized free $H_2$ molecules, $P/P_0$ is the ratio of system hydrogen gas pressure (2000 bar) to atmospheric pressure (1 bar), and RT is the gas constant multiplied by temperature (100 K). The favored occupancy number for guest molecules in each cage was determined by comparing association energies for different numbers of guest molecules.

Free volume calculations for the type-II hydrate were performed using the algorithm of Voorintholt et al.[30] and the Materials Studio software package.[31] Van der Waal radii for water molecule atoms were taken from the solvent-based optimizations of Stefanovich and Truong.[32] The guest hydrogen molecules were modeled by two connected spheres of radius 1.0 Å. Various radii for solvent probe atoms were used to display the cavity geometries.

## 3. RESULTS AND DISCUSSION

### 3.1. Unit Cell Optimization

After optimization of the type II hydrate clathrate unit cell, it was found that the PW91 density functional predicts an optimal lattice constant of 16.95 Å, only slightly smaller than the experimental value of 17.31 Å near room temperature. The binding energy per water molecule, not including zero point correction, is 0.71 eV (16.37 kcal/mol). This value is very similar to the 0.72 eV (16.61 kcal/mol) binding energy for ice Ih predicted by Feibelman.[33] Thus, despite the more open structure of the clathrate hydrate compared to ice Ih, they are similar in stability, which underscores the viability of clathrate hydrate structures. The optimized OtH bond lengths are $1.015 \pm 0.006$ Å, which are longer than the OtD bond length in ice Ih (0.975 Å), but well within other O–H bond lengths.

### 3.2. Structure of $H_2$ Inside Isolated Cages

The small (D-$5^{12}$) and large (H-$5^{12}6^4$) clathrate cages extracted from the optimized type II hydrate clathrate unit cell, with $n = 1$ and $n = 4$ $H_2$ occupancies, are shown in Figure 1. Table I gives the structural information for the optimized $H_2$ molecules, including the H–H bond lengths, the distances from the center of the cage (cm) to the $H_2$ molecule ($H_2$ cm), and the distances between $H_2$

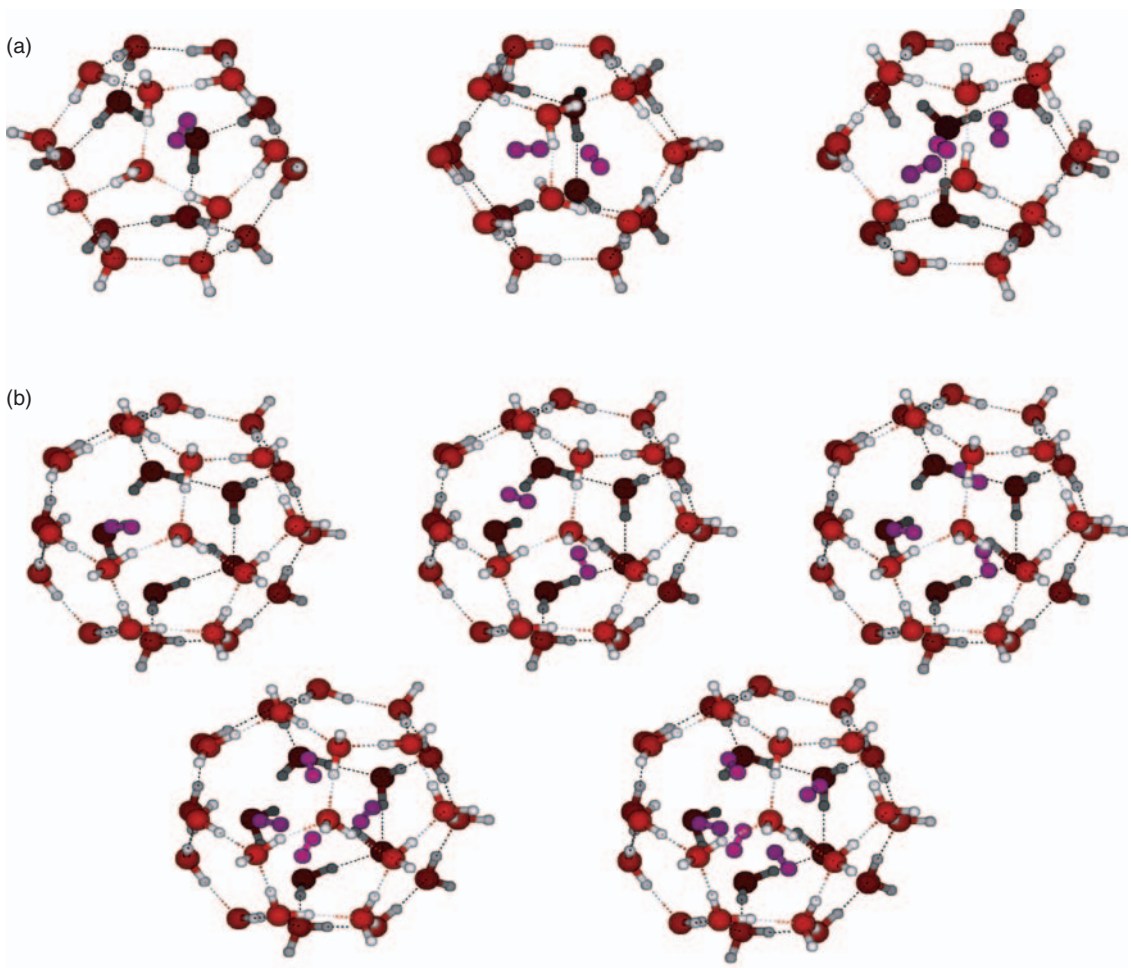


**Fig. 1.** Optimized $H_2$ guest molecules in isolated (a) small (D-512) and (b) large (H-51264) clathrate cages with increasing number of $H_2$ guests. The hydrogen bonding networks of the two cages are shown by dotted lines. For clarity, the guest $H_2$ molecules are shown in purple.

**Table I.** Structural properties of $nH_2$ optimized[a] in rigid clathrate cages.

| Number of associated $H_2^b$ | *Avg r* (H–H) Å | *Avg r* (cm–$H_2$ cm)[c, d] Å | *Avg r* ($H_2$ cm–$H_2$ cm)[d] Å |
|---|---|---|---|
| $1H_2 + \boldsymbol{S} = 1H_2@\boldsymbol{S}$ | 0.746 | 0.78 | NA |
| $2H_2 + \boldsymbol{S} = 2H_2@\boldsymbol{S}$ | 0.742 | 1.26 | 2.51 |
| $3H_2 + \boldsymbol{S} = 3H_2@\boldsymbol{S}$ | 0.737 | 1.49 | 2.57 |
| $1H_2 + \boldsymbol{L} = 1H_2@\boldsymbol{L}$ | 0.747 | 1.74 | NA |
| $2H_2 + \boldsymbol{L} = 2H_2@\boldsymbol{L}$ | 0.744 | 1.65 | 3.18 |
| $3H_2 + \boldsymbol{L} = 3H_2@\boldsymbol{L}$ | 0.743 | 1.85 | 3.05 |
| $4H_2 + \boldsymbol{L} = 4H_2@\boldsymbol{L}$ | 0.743 | 1.86 | 3.01 |
| $5H_2 + \boldsymbol{L} = 5H_2@\boldsymbol{L}$ | 0.742 | 1.98 | 3.09 |

[a]Guest $H_2$ positions were fully optimized inside the rigid cages at the rB3LYP/6-311G level of theory (see Fig. 1). [b]$\boldsymbol{S}$ indicates the small (D-$5^{12}$) cage and $\boldsymbol{L}$ indicates the large (H-$5^{12}6^4$) cage. [c]Cm is the center of mass of the cage. [d]$H_2$ cm is the center of mass of the H–H bond.

molecules. The optimized geometries of the guest hydrogen clusters found in this work are similar to the geometries described in the earlier *ab initio* work by Patchkovskii and Tse.[4]

The Optimized H–H Bond Lengths are ∼1% longer than the bulk gas length of 0.741 Å, with the exception of the three-fold occupied small cage. At this loading, the average H–H bond length decreases to 0.737 Å, indicating a strong repulsive force due to crowding inside the cage. When clusters of $H_2$ molecules are optimized outside of the cage, the H–H bond lengths were consistently 0.742 Å, implying that the guest $H_2$ molecules inside the cages experience little repulsive forces.

To accommodate multiple occupancies in the small (D-$5^{12}$) cage, the distance between the $H_2$ molecules decreased by 15–18% compared to the same occupancy inside the large (H-$5^{12}6^4$) cage (see Table I). This result is consistent with the distances reported in earlier MD simulations ($H_2$ cm–$H_2$ cm distances of 3.0 Å and 2.65 Å for the large and small cages, respectively).[6] In addition, the distance between the $H_2$ molecules in the four-fold occupied large cage, 3.01 Å, closely reproduces the experimental $D_2$ distance value of 2.93 Å.[5] This decrease in distance is further evidence of the repulsive forces, which destabilize multiple occupancies in the small cage.

The major difference in $H_2$ geometry between this and the earlier ab initio results are found with a single $H_2$ guest molecule in the small (D-$5^{12}$) cage. Patchkovskii and Tse reported an energy minimum for $H_2$ occurring at 1.1 Å from the center of the cage.[4] In this study, the $H_2$ molecule is much closer to the center (0.78 Å) of the cage. Two significant changes were made in this study: level of theory and the clathrate cage structure. Patchkovskii and Tse used the smaller 3-21G(p) basis set, a split-valence double-zeta basis set with polarization functions, and fixed OtH bond lengths at 1.0 Å. Using the smaller basis set with optimized O–H bond lengths, we found the same energy minimum. Thus, the 1.1 Å minimum reported earlier seems to be a consequence of the smaller basis.

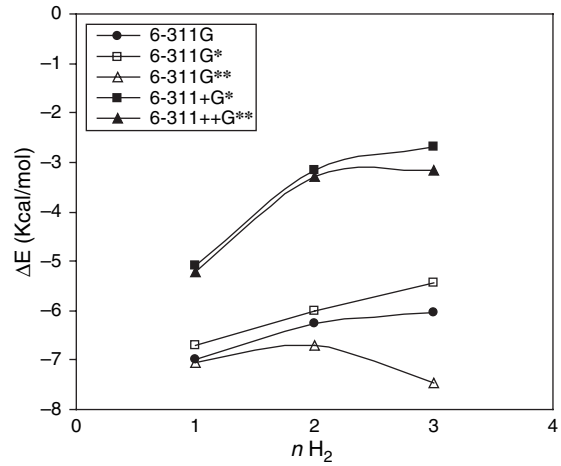


**Fig. 2.** Association energies (ΔE) as a function of guest $H_2$ occupancy in the small (D-512) cage for $H_2$ gas pressure of 2000 bar, $T = 250$ K. All calculations were performed at the MP2 level of theory. The basis set is given in the legend.

### 3.3. *Ab Initio* Association Energies

Figure 2 shows the energies for association of small water cages loaded with varied number of $H_2$ at the experimental pressure of 2000 bar and temperature of 250 K. All calculations used the MP2 method. Association energy converges at the large 6-311+G* basis set, which is a split-valence triple-zeta basis set with polarization and diffuse functions. At this level of theory, the association energy of the small (D-$5^{12}$) cluster increases to significantly less favorable values after the first guest $H_2$ molecule has been added. Thus, the optimal occupancy of the small (D-$5^{12}$) cage is one $H_2$ guest molecule. As evident from Figure 3, this is not the case for the large (H-$5^{12}6^4$) cage. The association energy of this cage shows a decrease in energy to

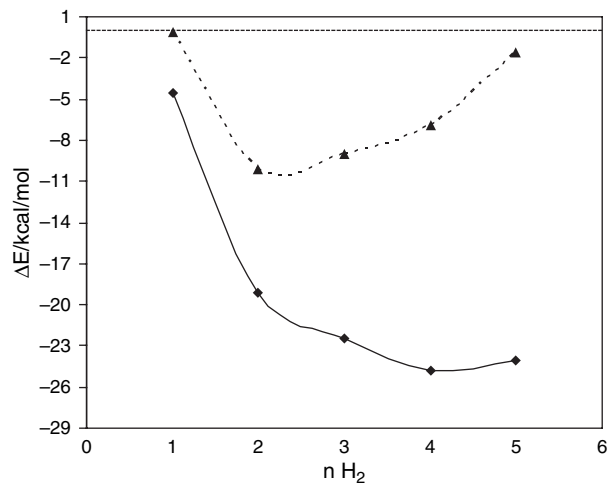


**Fig. 3.** Association energies (ΔE) as a function of guest $H_2$ occupancy in the large (H-51264) cage at $H_2$ gas pressures of 1 bar (dotted line) and 2000 bar (solid line), $T = 250$ K. All calculations were performed at the MP2/6-311+G* level of theory.

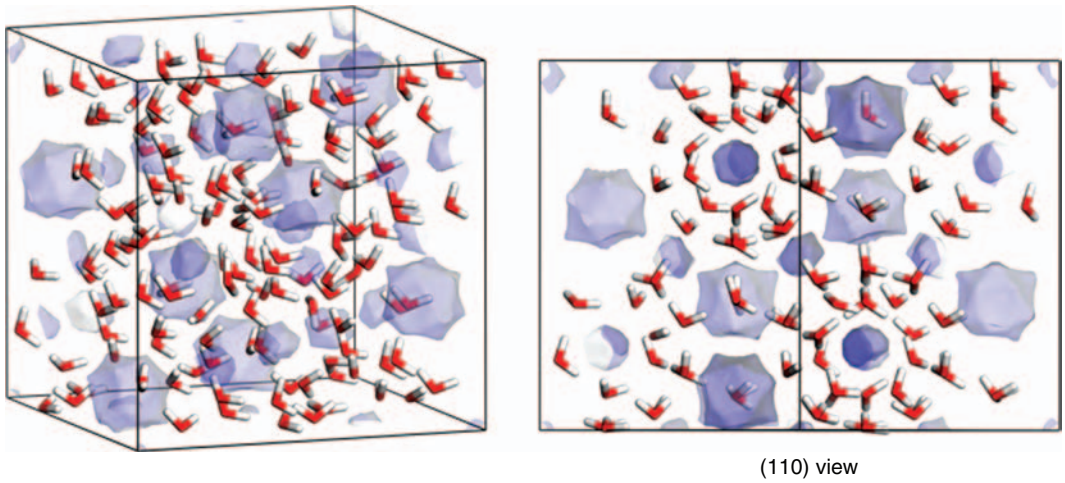


**Fig. 4.** Free volume inside the optimized type-II clathrate hydrate with no guest $H_2$ molecules. A 1.4 Å radius probe atom was used to generate the $H_2$-accessible surfaces. The occupied volume for the host water molecules is 4817 Å$^3$, while the available cavity volume for the guest molecules is 255 Å$^3$ with a surface area of 573 Å$^2$.

more favorable values when more than one $H_2$ molecule is placed inside the cage (see Fig. 3). At ambient pressure (1 bar), the large cage favors a double $H_2$ occupancy (dashed line), while at the experimental pressure (2000 bar), the favored occupancy increases to four $H_2$ molecules (solid line). Lokshin[5] showed similar changes in the occupancy of $D_2$ guest molecules in the clathrate type-II structure based on neutron diffraction experiments.

### 3.4. Available Volume

The available volume inside the cage alone will restrict the occupancy. Figure 4 provides two views of the available volume within the type-II clathrate; both views clearly exhibit the two different-sized cavities for the two cages. The surfaces represent the trace of the center of a spherical probe of radius 1.4 Å onto the hydrogen-bonded network of host water molecules. The non-spherical geometries associated with both small (D-$5^{12}$) and large (H-$5^{12}6^4$) volumes indicate the number of coordinating oxygens. The (110) view of the solvation surface best displays the relationship of the small to large cavities within the unit cell of the hydrate. Only two of the small cavities are fully coordinated entirely within the unit cell representation of the structure.

Van der Waal surfaces for the abstracted representations of the two cavities from structure II hydrate with their optimized hydrogen molecule positions are presented in Figure 5. The hydrogen molecules are represented by opaque surfaces and indicate the molecular disposition and coordination within each cavity. It is possible for three hydrogen molecules to occupy the small cavity while five would fill the larger cavity. Careful examination of the semi-transparent van der Waal surface for the water molecules shows the close contact of the guest hydrogen molecules with the equivalent surface associated with the

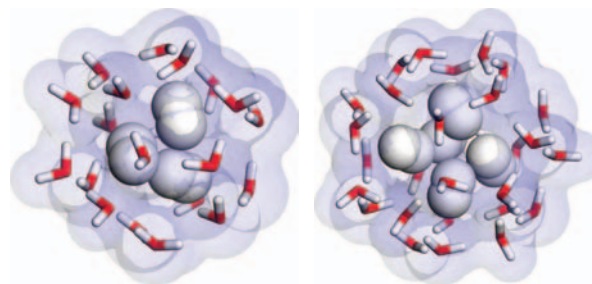

**Fig. 5.** Van der Waals surfaces for the isolated clathrate cavities (small D–$5^{12}$ on left, large H–$5^{12}6^4$ on right) with their maximum number of guest hydrogen molecules considering free volume effects only (three $H_2$ in the small, and five $H_2$ in the large cavities). Geometries of the guest hydrogen molecules were optimized. The external surface representation is unimportant.

host water molecules. If volume and geometry were the only factor, the occupancy of the cages would be significantly larger. Therefore, repulsive forces between the guest hydrogen molecules and between the guest hydrogen and water molecules of the cage must play a significant role in the occupancy of these clusters, which is also supported by recent observations from *ab initio* molecular dynamics simulations of hydrogen molecule solvated by bulk water.[34, 35]

## 4. CONCLUSIONS

It has been suggested that the MD simulations obtained a single $H_2$ occupancy in the small cage because their model allowed flexibility of the cage and included cooperative effects of the neighboring cages.[6] This work has demonstrated that neither property affects the occupancy of the small cage and that *ab inito* quantum chemical calculations predict the single occupancy of the small cage based on

association energies, even without flexibility or long-range cooperative interactions considered in the model.

**Acknowledgments:** We thank Dr. D. Sabo for useful discussions. This work was supported by Sandia's LDRD program. Sandia is a multi-program laboratory operated by Sandia Corporation, a Lockheed Martin Company, for the U.S. DoE NNSA under contract DE-AC04-94AL8500.

## References

**1.** W. L. Mao, H.-K. Mao, and A. F. Goncharove, *Science* 297, 2247 (**2002**).
**2.** V. V. Struzhkin, B. Militzer, W. L. Mao, H.-K. Mao, and R. J. Hemley, *Chem. Rev.* 107, 4133 (**2007**).
**3.** M. H. F. Sluiter, H. Hadachi, R. V. Belosludov, V. R. Belosludov, and Y. Kawazoe, *Materials Transactions* 45, 1452 (**2004**).
**4.** S. Patchkovskii and J. S. Tse, *PNAS* 100, 14645 (**2003**).
**5.** K. A. Lokshin, Y. Zhao, D. He, W. L. Mao, H.-K. Mao, R. J. Hemley, M. Lobanov, and M. Greenblatt, *Phys. Rev. Lett.* 93 (**2004**).
**6.** S. Alavi, J. A. Ripmeester, and D. D. Klug, *J. Chem. Phys.* 123, 024507 (**2005**).
**7.** H. E. J. King and E. A. Smelik, *Zeitschrift für Kristallographie* 211, 84 (**1996**).
**8.** R. T. Cygan, S. Guggenheim, and A. F. K. van Groos, *J. Phys. Chem. B* 108, 15141 (**2004**).
**9.** G. Kresse and J. Hafner, *Phys. Rev. B* 47, 558 (**1993**).
**10.** G. Kresse and Furthmuller, *Phys. Rev. B* 54, 11169 (**1996**).
**11.** G. Kresse and Furthmuller, *J. Comp. Mat. Sci.* 6, 15 (**1996**).
**12.** K. Burke, J. P. Perdew, and Y. Wang, Electronic Density Funtional Theory: Recent Progress and New Directions, Plenum (**1998**).
**13.** J. P. Perdew, Electronic Structure of Solids ′91; Akademie Verlag, Berlin (**1991**).
**14.** J. P. Perdew, K. Burke, and Y. Wang, *Phys. Rev* B 54, 16533 (**1996**).
**15.** J. P. Perdew, J. A. Chevary, S. H. Vosko, K. A. Jackson, M. R. Pederson, D. J. Singh, and C. Fiolhais, *Phys. Rev.* B 46 (**1992**).
**16.** J. P. Perdew, J. A. Chevary, S. H. Vosko, K. A. Jackson, M. R. Pederson, D. J. Singh, and C. Fiolhais, *Phys. Rev.* B 48 (**1993**).
**17.** D. Vanderbilt, *Phys. Rev. B* 41, 7892 (**1990**).
**18.** M. J. Frisch, G. W. Trucks, H. B. Schlegel, G. E. Scuseria, M. A. Robb, J. R. Cheeseman, J. A. J. Montgomery, T. Vreven, K. N. Kudin, J. C. Burant, J. M. Millam, S. S. Iyengar, J. Tomasi, V. Barone, B. Mennucci, M. Cossi, G. Scalmani, N. Rega, G. A. Petersson, H. Nakatsuji, M. Hada, M. Ehara, K. Toyota, R. Fukuda, J. Hasegawa, M. Ishida, T. Nakajima, Y. Honda, O. Kitao, H. Nakai, M. Klene, X. Li, J. E. Knox, H. P. Hratchian, J. B. Cross, V. Bakken, C. Adamo, J. Jaramillo, R. Gomperts, R. E. Stratmann, O. Yazyev, A. J. Austin, R. Cammi, C. Pomelli, J. W. Ochterski, P. Y. Ayala, K. Morokuma, G. A. Voth, P. Salvador, J. J. Dannenberg, V. G. Zakrzewski, S. Dapprich, A. D. Daniels, M. C. Strain, O. Farkas, D. K. Malick, A. D. Rabuck, K. Raghavachari, J. B. Foresman, J. V. Ortiz, Q. Cui, A. G. Baboul, S. Clifford, J. Cioslowski, B. B. Stefanov, G. Liu, A. Liashenko, P. Piskorz, I. Komaromi, R. L. Martin, D. J. Fox, T. Keith, M. A. Al-Laham, C. Y. Peng, A. Nanayakkara, M. Challacombe, P. M. W. Gill, B. Johnson, W. Chen, M. W. Wong, C. Gonzalez, and J. A. Pople, Gaussian 03; C.02 ed. Gaussian, Inc: Wallingford CT (**2004**).
**19.** A. D. Becke, *J. Chem. Phys.* 98, 5648 (**1993**).
**20.** C. Lee, W. Yang, and R. G. Parr, *Phys. Rev. B* 37, 785 (**1988**).
**21.** R. Krishnan, J. S. Binkley, R. Seeger, and J. A. Pople, *J. Chem. Phys.* 72, 650 (**1980**).
**22.** A. D. McLean and G. S. Chandler, *J. Chem. Phys.* 72, 5639 (**1980**).
**23.** C. Moller and M. S. Plesset, *Phys. Rev.* 46, 618 (**1934**).
**24.** K. D. Dobbs and W. J. Hehre, *J. Comp. Chem.* 7, 359 (**1986**).
**25.** K. D. Dobbs and W. J. Hehre, *J. Comp. Chem.* 8, 861 (**1987**).
**26.** K. D. Dobbs and W. J. Hehre, *J. Comp. Chem.* 8, 880 (**1987**).
**27.** J. S. Binkley, J. A. Pople, and W. J. Hehre, *J. Am. Chem. Soc.* 102, 939 (**1980**).
**28.** M. S. Gordon, J. S. Binkley, J. A. Pople, W. J. Pietro, and W. Hehre, *J. Am. Chem. Soc.* 104, 2797 (**1982**).
**29.** W. J. Pietro, M. M. Francl, W. J. Hehre, D. J. Defrees, J. A. Pople, and J. S. Binkley, *J. Am. Chem. Soc.* 104, 5039 (**1982**).
**30.** R. Voorintholt, M. T. Kosters, G. Vegter, G. Vriend, and W. G. J. Hol, *J. Molec. Graphics* 7, 243 (**1989**).
**31.** Accelrys, Release 4.4 ed.; Accelrys Software, Inc., San Diego, CA (**2008**).
**32.** E. V. Stefanovich and T. N. Truong, *Chem. Phys. Lett.* 244, 65 (**1995**).
**33.** Feilbelman, *Science* 295, 8075 (**2002**).
**34.** D. Sabo, S. B. Rempe, J. A. Greathouse, and M. G. Martin, *Molecular Simulation* 32, 269 (**2006**).
**35.** D. Sabo, S. Varma, M. Martin, and S. B. Rempe, *J. Phys. Chem. B* 112, 867 (**2008**).

Received: 8 December 2009. Accepted: 4 January 2010.